Biol. Cybern. 85, 281–291 (2001)

Biological Cybernetics

The effect of subthreshold prepulses on the recruitment order in a nerve trunk analyzed in a simple and a realistic volume conductor model

Kirsten E. I. Deurloo, Jan Holsheimer, Piet Bergveld

Department of Electrical Engineering, Institute for Biomedical Technology, University of Twente, P.O. Box 217, 7500 AE Enschede, The Netherlands

Received: 15 May 2000 / Accepted in revised form: 9 February 2001

Abstract. The influence of subthreshold depolarizing prepulses on the threshold current-to-distance and the threshold current-to-diameter relationship of myelinated nerve fibers has been investigated. A nerve fiber model was used in combination with both a simple, homogeneous volume conductor model with a point source and a realistic, inhomogeneous volume conductor model of a monofascicular nerve trunk surrounded by a cuff electrode. The models predict that a subthreshold depolarizing prepulse will desensitize Ranvier nodes of fibers in the vicinity of the cathode and thus cause an increase in the threshold current of a subsequent pulse to activate these fibers. If the increase in threshold current of the excited node is large enough, the excitation will be accompanied by a strong hyperpolarization of adjacent nodes, preventing the propagation of action potentials in these fibers. As fibers close to the electrode are more desensitized by prepulses than more distant ones, it is possible to stimulate distant fibers without stimulating such fibers close to the electrode. Moreover, as larger fibers are more desensitized than smaller ones, smaller fibers have lower threshold currents than larger fibers up to a certain distance from the electrode. The realistic model has provided an additional condition for the application of this method to invert nerve fiber recruitment, i.e., real or virtual anodes should be close to the cathode. When using a cuff electrode for this purpose, in the case of monopolar stimulation the cuff length (determining the position of the virtual anodes) should not exceed twice the internodal length of the fibers to be blocked. Similarly, the distance between cathode and anodes should not exceed the internodal length of these fibers when stimulation is to be applied tripolarly.

Correspondence to: J. Holsheimer
(Fax: +31-53-4892287, e-mail: j.holsheimer@el.utwente.nl)

1 Introduction

Functional electrical stimulation (FES) can be used to restore motor functions in neurologically impaired patients by artificially stimulating their nervous system. When the peripheral neuromuscular system is still intact, muscles can be activated by electrical stimulation of the motor nerve fibers innervating these muscles. To produce proper muscle contractions it is necessary for the activation of motor nerve fibers to be controlled with respect to their position in a nerve trunk and their diameter. Different techniques have been developed to activate selectively nerve fibers of a given diameter range or nerve fibers in a limited part of a peripheral nerve trunk, particularly by the use of a nerve cuff electrode (Grill and Mortimer 1995).

Most research on size-selective stimulation has been focused on the development of methods to activate small myelinated fibers without activating the larger ones. The threshold stimulus current is inversely related to the fiber caliber. Due to their larger internodal lengths, large fibers are activated at lower stimulus currents than smaller ones ('inverse' recruitment order, as compared to physiological recruitment) (McNeal 1976). For various applications, however, smaller fibers within the α-motor range (10–18 μm) should be activated first, e.g., to obtain a graded contraction of limb muscles. In sacral root stimulation for bladder control, the small (parasympathetic) fibers (2–5 μm) should be activated exclusively. To achieve this goal, nerve cuffs with a tripolar configuration of ring-shaped contacts (central cathode) have been applied. Near the cathode all fibers are excited, whereas the propagation of action potentials evoked in primarily the large fibers is blocked near the anodes, so that only action potentials elicited in the smaller fibers reach their target muscle (Fang and Mortimer 1991; Rijkhoff et al. 1994).

Spatial selectivity refers to the ability to stimulate discrete groups of nerve fibers in a limited region without stimulating nerve fibers in neighboring regions. Stimulus-induced transmembrane potential changes are largest in nerve fibers close to the stimulating electrode.

Therefore, the stimulus current required to excite nerve fibers close to the electrode is smallest and this current increases approximately proportional to the square of the distance between the electrode and the nerve fiber. Usually, multi-contact (spiral) nerve cuff electrodes are placed around the nerve trunk and by using different contact configurations driven by one or more pulse generators, fibers in the periphery of the nerve trunk can be activated selectively (Veraart et al. 1993; Grill and Mortimer 1996; Deurloo et al. 1998). A combination of controlled smaller fiber selectivity and spatial selectivity, however, is hard to obtain (Goodall et al. 1996).

As described above, the two basic relations of the stimulus current needed for nerve fiber activation are: (1) the current is inversely related to the caliber of the myelinated nerve fiber and (2) the current increases approximately proportional to the square of the distance between the nerve fiber and the stimulating electrode (which is generally the cathode). These two relations imply that with a given stimulus amplitude, larger fibers will be activated up to a larger distance from the cathode than smaller fibers. Therefore, larger fibers will be activated in a larger area of a nerve trunk than smaller fibers. Furthermore, fiber recruitment starts near the cathode and spreads both tangentially and radially towards the center of the trunk (Deurloo et al. 1998).

Due to the threshold current-to-distance relationship, it would be impossible to activate only nerve fibers positioned centrally in a nerve trunk with a cuff electrode, as has been noted by Veltink et al. (1989). Sassen and Zimmermann (1973) observed in experiments that the activation of large nerve fibers by a cathodal stimulating pulse can be prevented when a long, subthreshold, depolarizing prepulse is applied immediately before the stimulating pulse. Grill and Mortimer (1995, 1997) used this method to activate selectively fibers more centrally in a nerve trunk. They have shown by computer modeling that rectangular, subthreshold, depolarizing prepulses generate a transient decrease in neural excitability of primarily large nerve fibers close to the cathode, and thus an increase in the threshold current of a subsequent stimulus pulse required to activate these fibers. In this way, an inversion of the threshold current-to-distance relationship up to some distance from the cathode could be obtained, which allows the selective stimulation of primarily large nerve fibers distant from the cathode. Grill and Mortimer have also shown that up to some distance from the cathode, a stepped prepulse allows stimulation of smaller nerve fibers at lower stimulus amplitudes than larger nerve fibers.

Selective activation of nerve fibers distant from the cathode can also be obtained by monopolar cathodal stimulation, when currents of 2–3 times the threshold stimulus are used, inducing 'surround block' in primarily large fibers close to the cathode (Ranck 1975). The blocking threshold (due to strong hyperpolarization of neighboring nodes of Ranvier) has a similar relation to fiber caliber and distance from the cathode as the excitation threshold. However, this method requires relatively high currents.

Grill and Mortimer (1997) studied the effect of prepulses in a simple, homogeneous, isotropic volume conductor model with a cathodal point source. We have performed simulations using both this simple volume conductor model and a more realistic, inhomogeneous, anisotropic model representing a monofascicular nerve in a cuff. Using these models we investigated in detail the influence of subthreshold depolarizing prepulses on myelinated nerve fibers. First, we used the simple volume conductor model and compared the results with those obtained by Grill and Mortimer (1997). Next, we used the more realistic volume conductor model and simulated the effects of monopolar and longitudinal tripolar stimulation, the latter with different contact separations. Due to several differences between the simple and the more realistic model (contact area, position of (virtual) anodes, 3D potential distribution), the results differed as well.

2 Methods

The electrical behavior of mammalian myelinated nerve fibers was analyzed in two different 3D volume conductor models to determine the effect of subthreshold depolarizing prepulses on the relationship between the threshold current and the distance between the electrode and a nerve fiber. A simple, homogeneous volume conductor model with a point source was used, as well as a more realistic, inhomogeneous nerve and cuff model.

2.1 Homogeneous volume conductor model

A 3D homogeneous, isotropic, infinite volume conductor model with a current point source at its center was used. The steady-state electrical potentials in this model were solved analytically according to:

$$V = I/4\pi\sigma r \tag{1}$$

with V the potential at the point of observation [V], r the distance of this point from the point source [m], I the injected current [A], and σ the material conductivity [Ω^{-1} m^{-1}]. The value of σ (1.818 Ω^{-1} m^{-1}) was the same as used by Grill and Mortimer (1995, 1997).

2.2 Realistic volume conductor model

The 3D inhomogeneous volume conductor model represents a monofascicular nerve trunk surrounded by a cuff electrode. A transverse section of the model is shown in Fig. 1. The nerve fascicle had a length of 23 mm and a diameter of 1.7 mm, and was surrounded by a 50-μm layer of perineurium and a 50-μm layer of epineurium. The cuff had an inner diameter of 2 mm, and was 0.25 mm thick and 10 mm long. The 50-μm space between nerve trunk and cuff was filled with saline. The cuff was surrounded by saline and the outermost layer of the model was a low-conductivity boundary

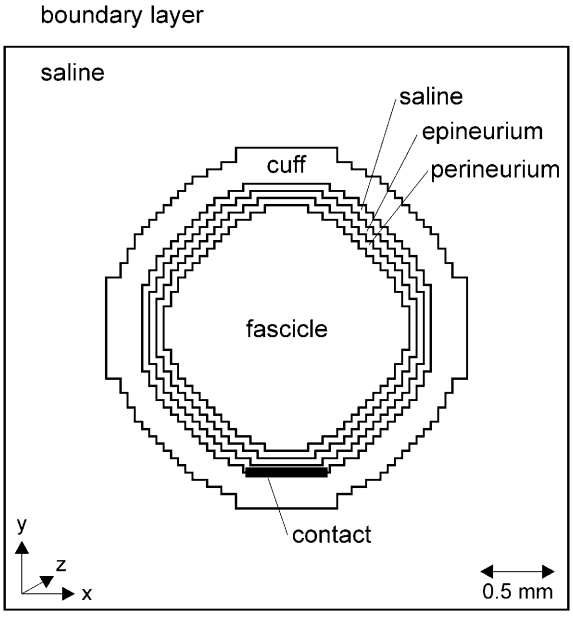

Fig. 1. Transverse section of the 3D volume conductor model of a monofascicular nerve trunk surrounded by a cuff electrode

layer. The potential at the border of the model was set to zero to represent a distant ground. In case of monopolar (cathodal) stimulation, the border of the model served as the distant anode. Electrode dot contacts (0.5×0.5 mm) were modeled as current sources, and were placed on the inner surface of the cuff. The compartmental conductivities used in the model are presented in Table 1, and had the same values as in a previous modeling study (Deurloo et al. 1998).

To discretize the volume conductor model, a rectangular grid of variable size was used, with the smallest grid sizes near the contacts. The steady-state potential field was obtained by applying a finite difference method using Taylor series and solving the resulting set of linear equations by a Red-Black Gauss-Seidel iteration with variable overrelaxation. The model and the computational algorithm have been extensively described in previous papers (Struijk et al. 1992; Goodall et al. 1995; Deurloo et al. 1998).

Table 1. Conductivities of the 3D inhomogeneous volume conductor model compartments (Deurloo et al. 1998)

Model compartment	Conductivity σ (Ω^{-1} m^{-1})
Boundary layer	0.02
Saline	2.0
Cuff	0.0008
Epineurium	0.008
Perineurium	0.00336
Fascicle	0.08 (σ_x, σ_y) 0.5 (σ_z)

2.3 Nerve fiber model

A McNeal-type cable model (McNeal 1976) was used to simulate the stimulation of myelinated nerve fibers. Instead of the Frankenhaeuser-Huxley equations, describing the non-linear nodal membrane behavior of frog myelinated nerve fibers, the equations of Chiu (Chiu et al. 1979) based on experimental data from rabbit myelinated nerve fibers were used to include mammalian nonlinear membrane kinetics. Membrane parameters have been transformed to a temperature of 37 °C by Sweeney et al. (1987). A complete description of the fiber model and its parameters is presented in Appendix A. The parameter values are the same as used by Grill and Mortimer (1995, 1997).

All nodes of Ranvier were represented by a voltage-dependent sodium conductance, a (voltage-independent) leakage conductance, and a nodal capacitance. A voltage-dependent potassium conductance has not been incorporated because it has been shown that potassium channels are absent or scarce at nodes of Ranvier in myelinated fibers of rabbit sciatic nerve (Chiu et al. 1979). The internodal myelin sheath was assumed to be a perfect insulator (McNeal 1976).

2.4 Implementation of nerve fiber model and volume conductor models

Simulations with the nerve fiber model in combination with the homogeneous volume conductor model were performed on a PC. This model will be named 'simple model'. Nerve fibers were modeled using a 21-node cable model. The nerve fibers were positioned at different distances from the point source, which was placed in the plane perpendicular to the fiber axis at the central node of Ranvier (node 11). An iterative method was used to determine threshold currents generating an action potential characterized by a 70-mV depolarization of the membrane at the central node. To check whether the action potential was propagating, its occurrence was always determined at several nodes away from the central node.

Simulations with the nerve fiber model in combination with the realistic volume conductor model were performed on an HP 9000/730 workstation. This model will be named 'realistic model'. Nerve fibers were positioned at different distances from the cathode, with the central node of the fibers placed in the transverse plane at the center of the cathode, or with the nodes offset by half the internodal length. Threshold currents generating propagating action potentials during monopolar and longitudinal tripolar stimulation were determined as described for the simple model.

In both models, 10- and 20-μm diameter nerve fibers and pulse widths of 500 μs were used, as Grill and Mortimer (1995, 1997) did in their simple model. The geometric fiber parameters are given in Table 2. In Figs. 2, 4, and 5, the reduced membrane potential V_m has been plotted, where V_m is the deviation of the resting membrane potential.

Table 2. Geometric fiber parameters

	Simple model		Realistic model	
	Small	Large	Small	Large
Fiber diameter	10 μm	20 μm	10 μm	20 μm
Axon diameter	6 μm	12 μm	6 μm	12 μm
Nodal length	1.5 μm	1.5 μm	1.5 μm	1.5 μm
Internodal length	1 mm	2 mm	1 mm	2 mm
Fiber length	20 mm	40 mm	22 mm	20 mm
Number of nodes	21	21	23	11

3 Results

3.1 Simple model

The simple model was used to analyze the electrical behavior at different nodes of myelinated 10- and 20-μm nerve fibers when a single pulse with or without one or two prepulses was applied, and to compare the calculated threshold currents with those obtained by Grill and Mortimer (1997).

3.1.1 Single stimulating pulse. The depolarization or hyperpolarization of nodes of Ranvier is related to the distance to the cathode and the internodal distance (and thus the fiber size). For both 10- and 20-μm fibers, the steady-state depolarization/hyperpolarization of all nodes was determined by applying a single subthreshold constant current pulse. In Fig. 2, the steady-state nodal potentials (100 μs after stimulus pulse initiation) of the 10-μm fiber positioned 0.25 mm (Fig. 2a) and 1 mm (Fig. 2b) from the point source are shown for all nodes. It is shown that for the fiber positioned 0.25 mm from the point source, only the central node was depolarized while all other nodes were hyperpolarized, whereas for the fiber positioned 1 mm from the point source the central node and the two adjacent ones were depolarized and the other nodes were hyperpolarized.

Next, with single 500-μs rectangular stimuli, the current to generate a propagating action potential as a function of the distance between the point source and a nerve fiber of diameter 10 and 20 μm, respectively, was calculated. The results are shown in Fig. 3a. The lower two curves are the threshold currents for excitation of the central node. The current increased as the distance was increased, and stimulation of smaller diameter nerve fibers required larger stimulus currents than stimulation of larger diameter nerve fibers. The upper two curves show the threshold currents required for direct excitation of neighboring nodes.

When the amplitude of a 500-μs pulse was increased, three cases of temporal distributions of the transmembrane potentials could be distinguished. The excitation threshold of the central node of the 10-μm fiber positioned 0.25 mm from the point source was 0.153 mA. In Fig. 4a, it is shown that at this current the membrane of central node 11 was depolarized sufficiently to produce an action potential (during the pulse) which propagated to the adjacent nodes (12, 13, etc.). The blocking threshold for this fiber was 0.416 mA. At this current an action potential was produced at node 11, but due to the strong hyperpolarization of the adjacent nodes (10 and 12) and the pulse duration (which exceeds the action potential duration), the action potential was not propagated, as shown in Fig. 4b. Because the response of nodes 10 and 12 (as well as of nodes 9 and 13) is identical, only one is shown in Fig. 4.

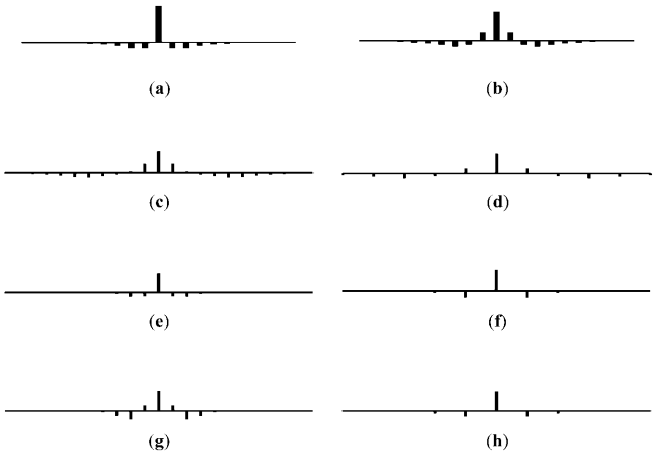

Fig. 2a–h. Steady-state reduced membrane potentials at all Ranvier nodes of a fiber model, 100 μs after initiation of a single subthreshold constant current pulse. **a,b** Simple model: 10-μm fiber positioned 0.25 mm **(a)** and 1 mm **(b)** from the point source, monopolar stimulation. **c–h** Realistic model, fibers positioned 0.15 mm from the cathode: **c** 10-μm and **d** 20-μm fiber, monopolar stimulation; **e** 10-μm and **f** 20-μm fiber, tripolar stimulation with 1.125 mm contact separation; **g** 10-μm and **h** 20-μm fiber, tripolar stimulation with 2.125 mm contact separation; internodal length of 10-μm and 20-μm fiber is 1 mm and 2 mm, respectively. Amplitude at central node is approximately 10 mV; depolarization upward, hyperpolarization downward

Increasing the current to 3.95 mA once more produced a propagating action potential which was initiated at node 12 (and 10), as shown in Fig. 4c. During the pulse, an action potential was generated at node 11 (not shown; maximum reduced membrane potential was 350 mV), but the neighboring nodes (10 and 12) were strongly hyperpolarized and this action potential was not propagated. The membrane potential of node 11 quickly decreased at the end of the pulse and at the same time raised the membrane potential of the neighboring (hyperpolarized) nodes just enough to reach the excitation level. As a result, another action potential was produced at node 12 (and 10), which propagated to the adjacent nodes (9 and 13).

The upper two curves of Fig. 3a are characterized by two regions in which the threshold current rises almost linearly (on a log scale), interrupted by larger increments. These regions are: (1) positions up to approximately 0.5 mm and 1.25 mm for 10- and 20-μm fibers, respectively; and (2) positions approximately 0.75–1.5 mm for 10-μm fibers and beyond approximately 1.5 mm for 20-μm fibers (not shown in Fig. 3a). When a single subthreshold pulse was applied to the 10- and 20-μm fibers in region 1, the steady-state nodal distribution of depolarization and hyperpolarization was the same as

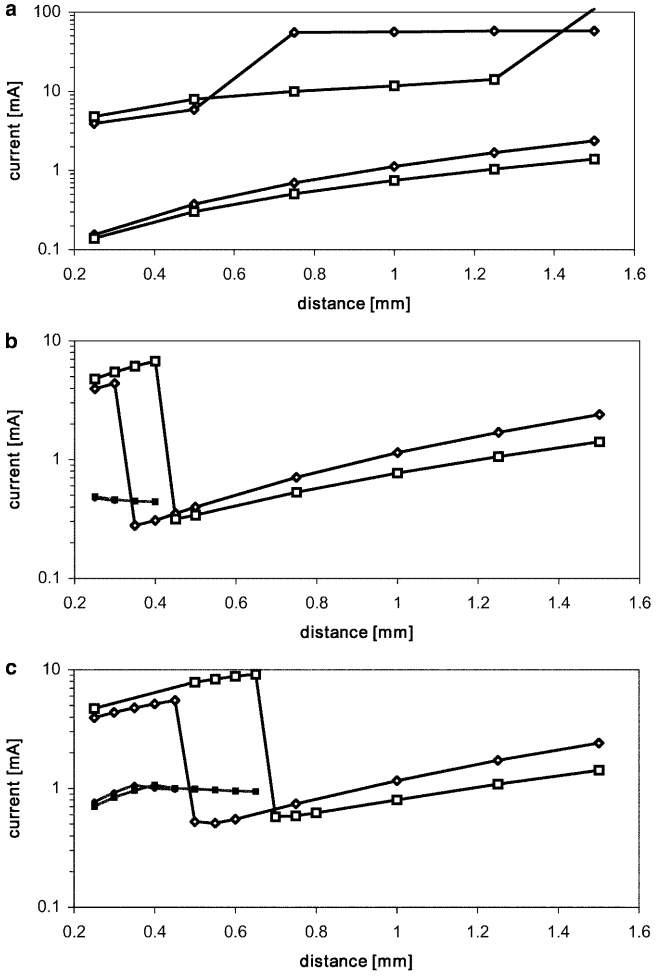

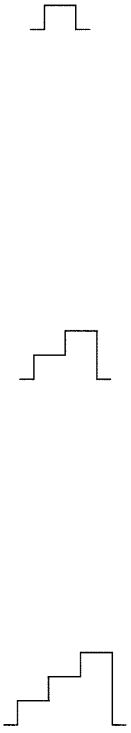

Fig. 3a–c. Threshold current (logarithmic scale) as a function of distance between point source and 10-μm (*open diamonds*) and 20-μm (*open squares*) diameter nerve fibers **a** 500-μs stimulus pulse; **b** 500-μs stimulus pulse preceded by a 500-μs depolarizing prepulse of 0.132 mA; **c** 500-μs stimulus pulse preceded by two depolarizing prepulses of 500 μs each and 0.132 mA and 0.264 mA, respectively. *Black squares* show the currents at which the transmembrane potential of the central node of fibers was elevated by 70 mV, but did not result in a propagating action potential

shown in Fig. 2a (central node depolarized, all other nodes hyperpolarized). At large stimulus currents, a propagating action potential may thus originate at the (hyperpolarized) nodes (10 and 12) on both sides of the central (depolarized) one (11), according to the mechanism illustrated in Fig. 4c. The corresponding (high) threshold currents for a 500-μs rectangular pulse are given by the upper curves in Fig. 3a.

In contrast, when a single subthreshold pulse was applied to the 10- and 20-μm fibers in region 2, the steady-state nodal distribution of depolarization and hyperpolarization was the same as shown in Fig. 2b (central node and the two adjacent nodes depolarized, other nodes hyperpolarized). At large stimulus currents, a propagating action potential may thus originate at the second nodes (9 and 13) on both sides of the central one (being the hyperpolarized nodes closest to central node 11). The mechanism (not shown) is similar to the one shown in Fig. 4c. The corresponding (high) threshold currents are given in Fig. 3a (upper curves). Note that at small distances (approximately 0.25–0.5 mm), the threshold currents for nodes 10 and 12 (next to the central one) of the 10-μm fiber were lower than those of the 20-μm fiber (due to their smaller internodal distance, and thus their smaller node-to-cathode distance).

3.1.2 Stimulating pulse with single depolarizing prepulse. In Fig. 3b the current-distance relationship is shown for 10- and 20-μm nerve fibers for a 500-μs rectangular stimulus pulse preceeded by a 500-μs depolarizing prepulse with an amplitude (0.132 mA) equal to 95% of the lowest excitation threshold (threshold current of a 20-μm fiber positioned 0.25 mm from the point source). For both fibers at a distance of 0.25–1.5 mm, the lowest current at which a propagating action potential was produced at an arbitrary node is indicated.

For 10- and 20-μm fibers up to approximately 0.35 mm and 0.45 mm from the point source, respectively, the prepulse elevated the threshold of the central node to such an extent that hyperpolarization of the adjacent nodes blocked action potential propagation. For example, in Fig. 5a (10-μm fiber positioned 0.25 mm from the point source) the prepulse was followed by a 0.471-mA stimulus pulse. It is shown that at this current level the transmembrane potential of central node 11 was elevated by only 70 mV (which is for rectangular stimulus pulses without a prepulse enough to produce a propagating action potential). The combination of the relatively small action potential and the hyperpolarization of the neighboring nodes precluded the generation of a propagating action potential. The black

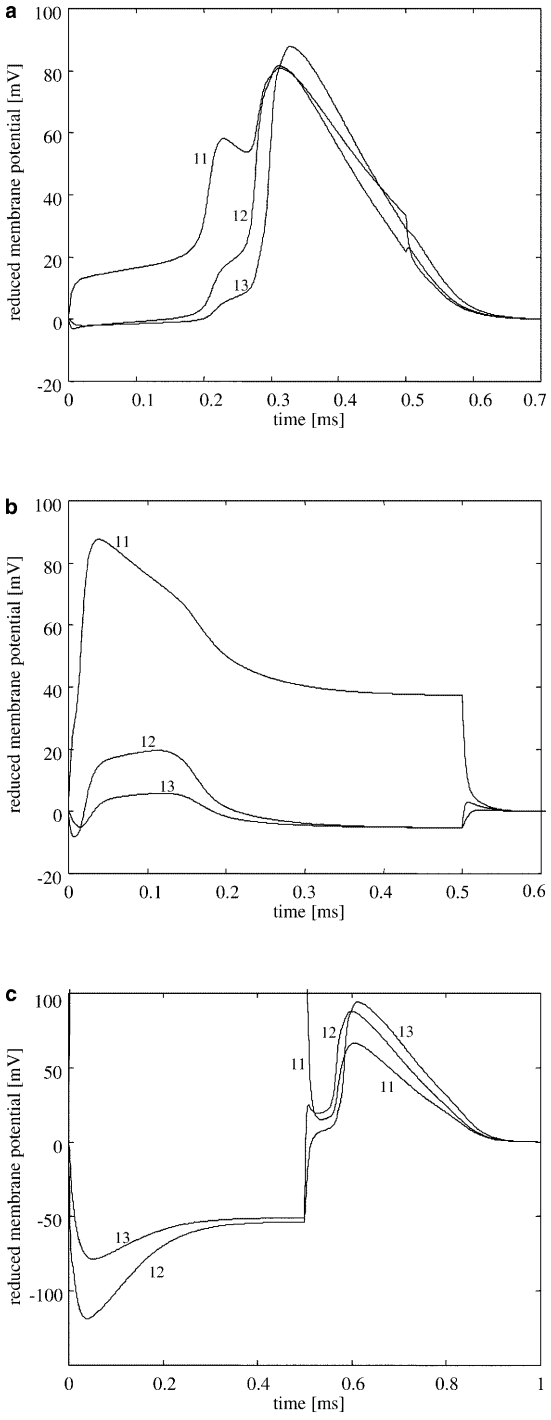

Fig. 4a–c. Reduced membrane potentials at nodes 11, 12, and 13 of a 10-μm nerve fiber positioned 0.25 mm from the point source; node 11 is the central node, and nodes 10 and 9 (not shown) have the same response as nodes 12 and 13, respectively: **a** 500-μs stimulus pulse of 0.153 mA (excitation threshold of node 11); **b** 500-μs stimulus pulse of 0.416 mA (blocking threshold of the fiber); **c** 500-μs stimulus pulse of 3.95 mA (maximum reduced membrane potential at node 11 was 350 mV)

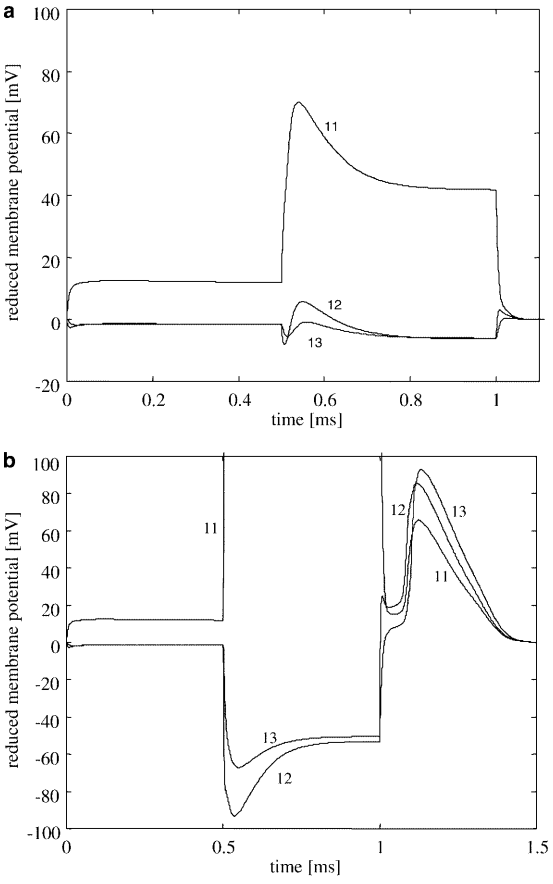

Fig. 5a,b. Reduced membrane potentials at nodes 11, 12, and 13 of a 10-μm nerve fiber positioned 0.25 mm from the point source; node 11 is the central node, and nodes 10 and 9 (not shown) have the same response as nodes 12 and 13, respectively: **a** 500-μs stimulus pulse of 0.471 mA preceded by a 500-μs depolarizing prepulse of 0.132 mA (note the reduced amplitude of the action potential (70 mV) at node 11); **b** 500-μs stimulus pulse of 3.93 mA preceded by a 500-μs depolarizing prepulse of 0.132 mA (a propagating action potential was initiated at nodes 10 and 12 at 0.1 ms after the stimulating pulse; the maximum reduced membrane potential at node 11 was 350 mV)

squares in Fig. 3b represent the current levels at which the transmembrane potential of the central node of both fibers was elevated by 70 mV, but did not result in a propagating action potential. Note that these current levels were almost identical for the 10- and 20-μm fibers, with the values of the 10-μm fiber being approximately 3% smaller. Furthermore, the elevated excitation currents of the 10-μm fiber (at a distance of 0.25 and 0.3 mm) were lower than the corresponding thresholds of the 20-μm fiber.

If the stimulus amplitude was increased to 3.93 mA (10-μm fiber positioned 0.25 mm from the point source), a propagating action potential was initiated about 0.1 ms after the end of the stimulus pulse at node 12, next to the central one. The corresponding behavior of the reduced membrane potentials of nodes 11, 12, and 13 of this fiber are presented in Fig. 5b.

3.1.3 Stimulating pulse with stepped depolarizing prepulse. The current-distance relationship for 10- and 20-μm nerve fibers after a 500-μs rectangular stimulus pulse preceeded by a double 500-μs depolarizing prepulse is shown in Fig. 3c. The amplitude of the first phase of the prepulse was equal to 95% of the lowest

excitation threshold (threshold current of a 20-μm fiber positioned 0.25 mm from the point source), and was 0.132 mA. The amplitude of the second phase was equal to 95% of the lowest excitation threshold after the first step of the prepulse (threshold of a 10-μm fiber positioned 0.35 mm from the point source, cf. Fig. 3b), and was 0.264 mA.

When using this double prepulse, 10- and 20-μm fibers positioned up to approximately 0.5 mm and 0.7 mm from the point source, respectively, could not be activated anymore at the central node. These fibers could, however, be activated at the nodes next to the central one, as with a rectangular stimulus pulse with or without a single depolarizing prepulse. The black squares in Fig. 3c represent the current levels defined in the same way as for the black squares in Fig. 3b.

3.2 Realistic model

The previous simulations have shown that in monopolar stimulation in a homogeneous medium, the distance between the central depolarized node and the nearest hyperpolarized one (or between the cathode and the virtual anodes) increases with increasing distance between a nerve fiber and the cathode. To investigate the effect of the distance between the cathode and the (virtual) anodes as an independent variable (as it is in most stimulation conditions), additional modelling was performed with unipolar stimulation and tripolar stimulation with different electrode spacings, using the realistic model of a nerve in a cuff.

3.2.1 Monopolar stimulation. Simulations were performed with a single dot cathode. The central node of the fibers was placed in the transverse plane at the center of the cathode. In Fig. 2, the steady-state nodal potentials (100 μs after initiation of a single subthreshold constant current pulse) of a 10-μm fiber (Fig. 2c) and a 20-μm fiber (Fig. 2d) positioned 0.15 mm from the cathode are shown. For both fibers, the central node and the two adjacent ones were depolarized while the other nodes were hyperpolarized. Maximum hyperpolarization occurred at the fifth (Fig. 2c) and third (Fig. 2d) nodes from the central one, corresponding to the position of the virtual anodes at both ends of the cuff. Figures 6a and b show the current-distance relationship for 10- and 20-μm nerve fibers, respectively, after a 500-μs rectangular stimulus pulse (open markers) and after a 500-μs pulse preceeded by a 500-μs depolarizing prepulse (black markers). The amplitude of the prepulse was equal to 95% of the excitation threshold of the corresponding fiber positioned 0.15 mm from the cathode, which is at the periphery of the nerve fascicle. For both fibers, the effect of the prepulse is limited. The prepulse slightly increased the threshold of all fibers. Large fibers are affected more than small ones and fibers close to the cathode are affected more than more distant ones. However, small fibers still have higher threshold currents than larger ones and fibers close to the cathode still have lower threshold currents than more distant ones. Only the threshold current of the 20-μm fiber at a distance of 0.15 mm is elevated to the same level as that at 0.2 mm.

3.2.2 Tripolar stimulation. Simulations were performed with two longitudinal tripoles, consisting of a dot cathode in between two dot anodes. The dot contacts had a center separation of either 1.125 mm or 2.125 mm. The central node of the fibers was placed in the transverse plane at the center of the cathode. In Fig. 2, the steady-state nodal potentials of a 10-μm (Fig. 2e,g) and a 20-μm (Fig. 2f,h) fiber positioned 0.15 mm from the cathode are shown, 100 μs after initiation of a single subthreshold constant current pulse. In three cases, the central node was depolarized while the other ones were hyperpolarized. Only in Fig. 2g, the central node and the two adjacent ones were depolarized while hyperpolarization started at the second node from the central one.

In Fig. 6c–f, the current-distance relationships for 10- and 20-μm nerve fibers after a 500-μs rectangular stimulus pulse (open markers) and after a 500-μs pulse preceeded by a 500-μs depolarizing prepulse (black markers) are shown. In all figures the amplitude of the prepulse was equal to 95% of the excitation threshold of a 20-μm fiber positioned 0.15 mm from the cathode (at the boundary of the fascicle). The dashed lines show the current levels at which the transmembrane potential of the central node was elevated by 70 mV, but this did not result in a propagating action potential. The computer program did not allow the determination of the much higher thresholds to excite the neighboring nodes after their hyperpolarization (cf. Fig. 3b).

For the tripole with 1.125-mm contact separation, the central node of 20-μm fibers positioned up to approximately 0.4 mm (Fig. 6c) from the cathode, and 10-μm fibers positioned up to approximately 0.25 mm (Fig. 6d) from the cathode, could not be activated when using the prepulse. When the contact separation was increased to 2.125 mm, the threshold currents were reduced considerably. The central node of all 10-μm fibers could now be activated when using the prepulse (Fig. 6f), whereas the central node of 20-μm fibers positioned up to approximately 0.4 mm from the cathode could not be activated (Fig. 6e).

In Fig. 6g, the simulations of Fig. 6e were repeated with the nodes of the 20-μm fiber offset by half the internodal length (i.e., by 1 mm). The central node of fibers positioned up to approximately 0.35 mm from the cathode could not be activated when using the prepulse. Threshold currents were slightly increased. The current levels at which the transmembrane potential of the central node of those fibers was elevated by 70 mV, but did not result in a propagating action potential (dashed line), were strongly reduced.

In Fig. 6h, the simulations of Fig. 6d were repeated with the nodes of the 10-μm fiber offset by half the internodal length (i.e., by 0.5 mm). The central node of fibers positioned up to approximately 0.25 mm from the

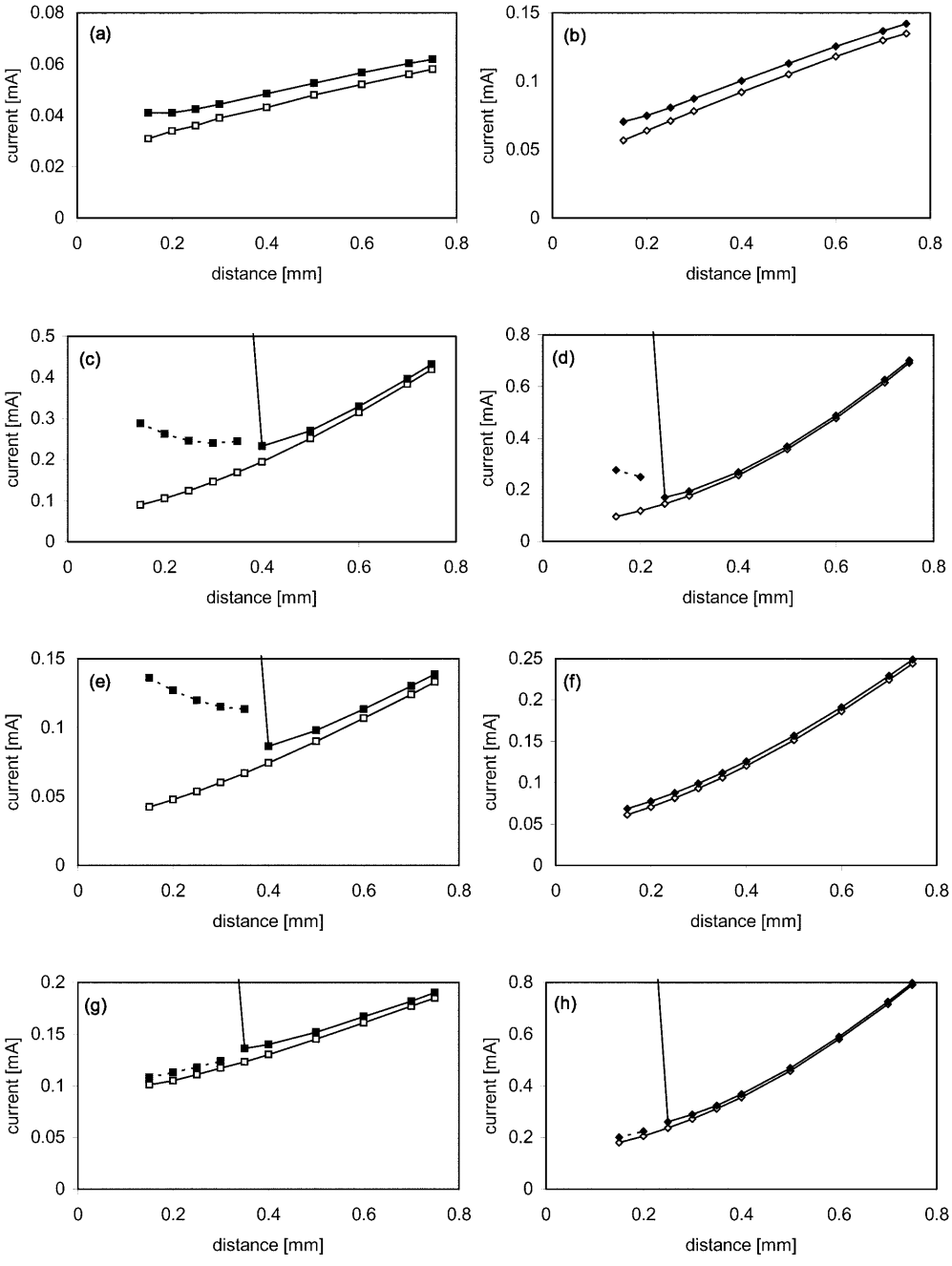

Fig. 6a–h. Threshold current as a function of fiber-to-cathode distance in realistic model for 500-μs stimulus pulses (*open symbols*) and 500-μs stimulus pulses preceded by 500-μs depolarizing prepulses (*filled symbols*): **a** 20-μm and **b** 10-μm fiber, monopolar stimulation; **c** 20-μm and **d** 10-μm fiber, tripolar stimulation with 1.125 mm contact separation; **e** 20-μm and **f** 10-μm fiber, tripolar stimulation with 2.125 mm contact separation; **g** as **e**, with nodes 1.0 mm offset; **h** as **d**, with nodes 0.5 mm offset. *Dashed lines* show the currents at which the transmembrane potential of the central node of fibers was elevated by 70 mV, but did not result in a propagating action potential

cathode (same fibers as in Fig. 6d) could not be activated when using the prepulse. Threshold currents were slightly increased and the dashed line was lowered.

4 Discussion

4.1 Simple model

In this modeling study the influence of subthreshold depolarizing prepulses on myelinated nerve fibers has been investigated. These prepulses have been initially used in experiments by Sassen and Zimmermann (1973) to block action potential propagation in large nerve fibers. Grill and Mortimer (1995, 1997) were the first to model the effect of these prepulses on the nonlinear conductance properties of nodal sodium channels, with the aim to change the neuronal recruitment order by electrical stimulation. Using a simple, homogeneous volume conductor model, they showed an inversion of the threshold current-to-distance relationship of fibers, allowing the selective stimulation of nerve fibers distant

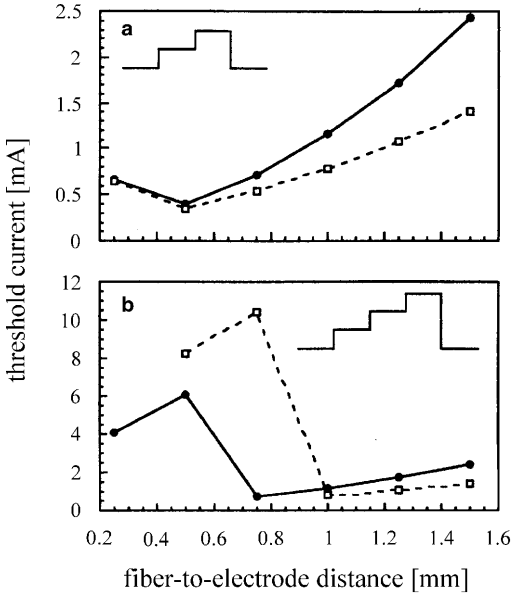

Fig. 7a,b. Threshold current as a function of distance between point source and 10-μm (*solid line*) and 20-μm (*dashed line*) nerve fiber models: **a** 500-μs stimulus pulse preceded by a 500-μs depolarizing prepulse of 0.131 mA; **b** 500-μs stimulus pulse preceded by two depolarizing prepulses of 500-μs each and 0.131 mA and 0.333 mA, respectively (from Grill and Mortimer 1997)

from the point source. Although we used exactly the same model, our results were different in some aspects.

Figure 7 shows the threshold current-to-distance relationships of 10- and 20-μm nerve fibers for a rectangular stimulus pulse preceeded by a single and a stepped prepulse, as presented by Grill and Mortimer (1997). In case of a single prepulse (Fig. 7a), thresholds for the two fiber diameters at distances of 0.5 mm and greater from the cathode are exactly the same as in our study (cf. Fig. 3b). Since Grill and Mortimer only looked at a intervals of 0.25 mm, they did not observe that the minimum of the curves is at approximately 0.35 and 0.45 mm for the 10- and 20-μm fiber, respectively (and not at 0.5 mm for both fiber diameters).

We observed that fibers closer to the point source cannot initiate a propagating action potential at the central node for two complementary reasons. First, the amplitude of the action potential at this node is reduced, due to the reduction of the nodal sodium conductance during the prepulse. Secondly, the threshold of this node is elevated to such an extent that its excitation is accompanied by a strong hyperpolarization of the adjacent nodes, thus blocking action potential propagation. Activation of these fibers may, however, occur after termination of the stimulus pulse at the nodes adjacent to the central one, but threshold currents for these nodes are higher by a factor of 15 or more. Although the excitation is elicited at previously hyperpolarized nodes, the underlying mechanism is different from anodal break excitation, which cannot be simulated with the model.

In contrast to our results, Grill and Mortimer (1995, 1997) showed that fibers close to the point source can be activated at the central node at an increased threshold current. They calculated that a 10-μm fiber positioned 0.25 mm from the point source is activated at a stimulus current of about 0.67 mA, as shown in Fig. 7a. We calculated that the blocking threshold of this fiber is equal to 0.416 mA (stimulated without prepulse). When this fiber is stimulated with a prepulse, a stimulus current of at least 0.471 mA is necessary to elevate the transmembrane potential of the central node to 70 mV above the resting potential, which is above the blocking threshold. It is, therefore, inconceivable that a propagating action potential can be generated with a stimulus current of 0.67 mA.

For the stepped prepulse waveform, Grill and Mortimer used 0.325 mA for the second phase of the prepulse, which is 95% of the threshold for activation of a 20-μm fiber positioned 0.5 mm from the point source after the first step of the prepulse. In Fig. 3b, it is shown that this fiber is not the most excitable one after a single prepulse. Using 0.325 mA for the second phase of the prepulse will, therefore, cause excitation of more excitable fibers during this phase of the prepulse (10-μm fiber at positions 0.35 and 0.4 mm and 20-μm fiber at position 0.45 mm). Grill and Mortimer did not observe this excitation, due to the large intervals in fiber-to-point source distances they used. We used 0.264 mA for the second phase of the prepulse, which is 95% of the threshold of the most excitable fiber after the first prepulse (10-μm fiber at position 0.35 mm).

Due to the differences in amplitude of the second phase of the prepulse, Figs. 3c and 7b can only be compared qualitatively. Grill and Mortimer stated that in two cases in Fig. 7b, the site of initiation of the action potential shifted from the central node to its neighbors (10-μm fiber at position 0.5 mm and 20-μm fiber at position 0.75 mm). We observed that for all points in Fig. 3b and c above 3 mA, the site of initiation of the action potential was at the node next to the central one. The 20-μm fiber positioned 0.25 mm from the point source, that could not be activated at any stimulus amplitude according to Grill and Mortimer, could, however, be activated in our simulations (at a stimulus current of 4.75 mA).

4.2 Realistic model

It has also been investigated whether the above-mentioned mechanisms, as analyzed in a homogeneous, isotropic, infinite medium, were valid in a more realistic, inhomogeneous, anisotropic nerve trunk and cuff model as well. When monopolar stimulation was applied, the effect of the prepulses was marginal. This is due to the position of the virtual anodes, being close to the cathode in the simple model, but rather distant in the realistic model, i.e., at both ends of the cuff. Since the modeled cuff was 10 mm long, maximum hyperpolarization occurred at several nodes away from the central node. The threshold current of the fibers was slightly elevated by the prepulse, but action potential propagation was not blocked, because the site of hyperpolarization was far away from the central node. The same result would be

obtained when a longitudinal tripolar combination with 5-mm contact spacing had been used for stimulation.

The different results we obtained when using the simple and the realistic model are related to the different geometrical and electrical properties of the volume conductor models (infinite, homogeneous, and isotropic vs. multicompartmental, inhomogeneous, and anisotropic). Although the results of the two models differ quantitatively, they are qualitatively similar.

Grill and Mortimer (1997) presented just one experimental example of the effect of a single prepulse on the recruitment of cat sciatic nerve fascicles with a nerve cuff electrode as measured by 3D ankle torques. The cuff length was at least 10 mm, although an exact value was not given. They used monopolar stimulation and stated that their results demonstrated that depolarizing prepulses allow the activation of a second recruited fascicle before stimulation of a first recruited fascicle. Our realistic model predicts that, when using monopolar stimulation in a cuff electrode of such a length, or longitudinal tripolar stimulation with a large contact spacing as compared to the internodal length, the use of prepulses will not invert the threshold current-to-distance relationship (cf. Fig. 6a,b,f).

When a longitudinal tripole with the smaller contact spacing (1.125 mm) was modeled, hyperpolarization started at the node next to the central one, and for fibers close to the cathode no propagating action potential could be initiated at the central node. For this narrow tripole, threshold currents were relatively high. Increasing the contact spacing to 2.125 mm decreased the threshold currents considerably, but the blocking effect of the prepulses vanished for the 10-μm fiber, as the node next to the central one was depolarized and hyperpolarization occurred at the second node.

Although fibers with a diameter of 20-μm have been modeled in this study, it has to be considered that the largest α-motor fibers in cat are only about 16 μm in diameter (Boyd and Davey 1968), and in man about 18 μm (Voorhoeve 1978). This implies that the effect on the largest fibers will be in between the results as shown for the 10- and 20-μm fibers.

Most simulations were done with the central node of the fibers placed in the same transverse plane as the center of the cathode, while in an actual nerve there will be a distribution of nodal positions relative to the cathode. Therefore, simulations were also performed with the nodes of the fibers offset by half the internodal length. It has been shown that under this condition the effect of the prepulses was still present and that fibers close to the cathode could not initiate a propagating action potential on the central node. Therefore, the effect as predicted by the realistic model will occur with any nodal position with respect to the cathode.

Grill (1999) reported that reversals in the recruitment order of nerve fibers as a function of fiber diameter and distance to the cathode may also be due to inhomogeneity or strong anisotropy of the tissues. He applied (monopolarly) single 100-μs pulses without any prepulse(s) to simple, analytical models: infinite, anisotropic, and homogeneous media, and semi-infinite, isotropic, and inhomogeneous media. Without applying prepulses however, we did not find any reversal when using the realistic model. Since both inhomogeneity, anisotropy, and geometry influence the imposed electric field and thus fiber recruitment, it is impossible to relate Grill's results to those from our realistic model.

Selective activation of nerve fibers distant from the electrode can also be obtained by blocking the action potentials in fibers closer to the electrode using single pulses with an amplitude several times larger than the excitation threshold (Ranck 1975). However, this 'surround block' needs relatively high currents and our modeling results indicate that the prepulse method requires less injected charge.

The modeling study presented, using both a simple and a realistic volume conductor model, has generally confirmed the conclusions of the study by Grill and Mortimer (1997) that subthreshold depolarizing prepulses allow the stimulation of distant fibers without stimulating such fibers close to the electrode, and that, up to a certain distance from the electrode, smaller fibers need less stimulus current than larger fibers. In addition, we have shown that the method is only effective when hyperpolarization occurs at nodes immediately neighboring the node closest to the cathode. This implies that for 10- to 20-μm fibers, the distance between cathode and (virtual) anodes should not exceed 1–2 mm. In case of monopolar stimulation with cuff electrodes, the cuff length (determining the position of the virtual anodes) should, therefore, not exceed 2–4 mm. Changing the distance between cathode and (virtual) anodes, in combination with the duration of the prepulses, will allow some control of the region in which fibers within a certain diameter range will not generate a propagating action potential.

Appendix A: The fiber model and its parameters at 37 °C

A.1 Fiber geometry

d	axon diameter [m]	$d = 0.6\mathrm{D}$
D	fiber diameter [m]	$L = 100\mathrm{D}$
L	internodal length [m]	
l	nodal width, 1.5 μm	
πdl	nodal area [m^2]	

A.2 Gating coefficients

$$\alpha_m = (363 \times 10^3 V + 126)/(1 + \exp\{-49 \times 10^{-3} - V)/5.3 \times 10^{-3}\})\ [\mathrm{ms}^{-1}]$$

$$\beta_m = \alpha_m/\exp\{(V + 56.2 \times 10^{-3}/4.17 \times 10^{-3}\}\ [\mathrm{ms}^{-1}]$$

$$\alpha_h = \beta_h/\exp\{(V + 74.5 \times 10^{-3})/5 \times 10^{-3}\}\ [\mathrm{ms}^{-1}]$$

$$\beta_h = 15.6/(1 + \exp\{(-56 \times 10^{-3} - V)/10 \times 10^{-3}\})\ [\mathrm{ms}^{-1}]$$

A.3 Gating variables

$\mathrm{d}m/\mathrm{d}t = \alpha_m(1-m) - \beta_m m \ [\mathrm{ms}^{-1}] \quad m(0) = 0.00331$
$\mathrm{d}h/\mathrm{d}t = \alpha_h(1-h) - \beta_h h \ [\mathrm{ms}^{-1}] \quad h(0) = 0.7503$

A.4 Constants

c_m specific membrane capacitance, 0.025 F/m^2
g_{Na} maximum sodium channel conductance, 14450 S/m^2
g_L nonspecific leakage channel conductance, 1280 S/m^2
ρ_a intra-axonal resistivity, 0.547 Ω m
V_L leakage equilibrium potential, −80.01 mV
V_{Na} sodium equilibrium potential, 35.64 mV
V_r resting membrane potential, −80 mV
V_m reduced membrane potential, $V_m = V - V_r$

A.5 Membrane currents

i_{Na} sodium current density [A/m^2]
$i_{Na} = g_{Na} m^2 h (V - V_{Na})$
i_L leakage current density [A/m^2]
$i_L = g_L (V - V_L)$
i_{ion} total ionic current density [A/m^2]
$i_{ion} = i_{Na} + i_L$
i_c capacitive current density [A/m^2]
$i_c = c_m \, \mathrm{d}V/\mathrm{d}t$
I_{mem} total nodal membrane current [A]
$I_{mem} = (i_{ion} + i_c)\pi dl$

References

Boyd IA, Davey MR (1968) Composition of peripheral nerves. Livingstone, Edinburgh

Chiu SY, Ritchie JM, Rogart RB, Stagg D (1979) A quantitative description of membrane currents in rabbit myelinated nerve. J Physiol (Lond) 292: 149–166

Deurloo KEI, Holsheimer J, Boom HBK (1998) Transverse tripolar stimulation of peripheral nerve: a modelling study of spatial selectivity. Med Biol Eng Comput 36: 66–74

Fang ZP, Mortimer JT (1991) Selective activation of small motor axons by quasitrapezoidal current pulses. IEEE Trans Biomed Eng 38: 168–174

Goodall EV, Kosterman LM, Holsheimer J, Struijk JJ (1995) Modeling study of activation and propagation delays during stimulation of peripheral nerve fibers with a tripolar cuff electrode. IEEE Trans Rehab Eng 3: 272–282

Goodall EV, De Breij F, Holsheimer J (1996) Position-selective activation of peripheral nerve fibers with a cuff electrode. IEEE Trans Biomed Eng 43: 851–856

Grill WM (1999) Modeling the effects of electric fields on nerve fibers: influence of tissue electrical properties. IEEE Trans Biomed Eng 46: 918–928

Grill WM, Mortimer JT (1995) Stimulus waveforms for selective neural stimulation. IEEE Eng Med Biol Mag 14: 375–385

Grill WM, Mortimer JT (1996) Quantification of recruitment properties of multiple contact cuff electrodes. IEEE Trans Rehab Eng 4: 49–62

Grill WM, Mortimer JT (1997) Inversion of the current-distance relationship by transient depolarization. IEEE Trans Biomed Eng 44: 1–9

McNeal DR (1976) Analysis of a model for excitation of myelinated nerve. IEEE Trans Biomed Eng 23: 329–337

Ranck JB (1975) Which elements are excited in electrical stimulation of mammalian central nervous system: a review. Brain Res 98: 417–440

Rijkhoff NJM, Holsheimer J, Koldewijn EL, Struijk JJ, van Kerrebroeck PEV, Debruyne FMJ, Wijkstra H (1994) Selective stimulation of sacral nerve roots for bladder control: a study by computer modeling. IEEE Trans Biomed Eng 41: 413–424

Sassen M, Zimmermann M (1973) Differential blocking of myelinated nerve fibers by transient depolarization. Pflügers Arch 341: 179–195

Struijk JJ, Holsheimer J, van der Heide GG, Boom HBK (1992) Recruitment of dorsal column fibers in spinal cord stimulation. IEEE Trans Biomed Eng 39: 903–912

Sweeney JD, Mortimer JT, Durand D (1987) Modeling of mammalian myelinated nerve for functional neuromuscular stimulation. Proc Annu Int Conf IEEE Eng Med Biol Soc 9: 1577–1578

Veltink PH, van Veen BK, Struijk JJ, Holsheimer J, Boom HBK (1989) A modeling study of nerve fascicle stimulation. IEEE Trans Biomed Eng 36: 683–692

Veraart C, Grill WM, Mortimer JT (1993) Selective control of muscle activation with a multipolar nerve cuff electrode. IEEE Trans Biomed Eng 40: 640–653

Voorhoeve PE (1978) Leerboek der neurofysiologie. Elsevier, Amsterdam, p 66